crystals

MDPI

Article

Hexagonal Nanocrystal Growth of Mg or Zn from Incorporation in GaN Powders Obtained through Pyrolysis of a Viscous Complex Compound and Its Nitridation

Erick Gastellóu [1,2,*], Rafael García [2], Ana M. Herrera [2], Antonio Ramos [2], Godofredo García [3], Gustavo A. Hirata [4], José A. Luna [3], Roberto C. Carrillo [5], Jorge A. Rodríguez [1], Mario Robles [1] and Yani D. Ramírez [6]

[1] División de Sistemas Automotrices, Universidad Tecnológica de Puebla (UTP), Antiguo Camino a la Resurrección 1002-A, Zona Industrial, Puebla 72300, Puebla, Mexico; jorge.rodriguez@utpuebla.edu.mx (J.A.R.); mario.robles@utpuebla.edu.mx (M.R.)
[2] Departamento de Investigación en Física, Universidad de Sonora (UNISON), Rosales y Colosio, C. De la Sabiduría, Centro, Hermosillo 83000, Sonora, Mexico; rafael.garcia@unison.mx (R.G.); ana.herrera@unison.mx (A.M.H.); antonio.ramos@unison.mx (A.R.)
[3] Centro de Investigacion en Dispositivos Semiconductores, Benemérita Universidad Autónoma de Puebla (BUAP), 14 Sur y Av. San Claudio, Puebla 72570, Puebla, Mexico; godofredo.garcia@correo.buap.mx (G.G.); jose.luna@correo.buap.mx (J.A.L.)
[4] Centro de Nanociencias y Nanotecnología, Universidad Nacional Autónoma de México (UNAM), Carr. Tijuana-Ensenada km107, C.I.C.E.S.E., Ensenada 22860, Baja California, Mexico; hirata@ens.cnyn.unam.mx
[5] Departamento de Física, Universidad de Sonora (UNISON), Rosales y Colosio, C. De la Sabiduría, Centro, Hermosillo 83000, Sonora, Mexico; roberto.carrillo@unison.mx
[6] Departamento de Investigación y Desarrollo, Universidad Tecnológica de Puebla (UTP), Antiguo Camino a La Resurrección 1002-A, Zona Industrial, Puebla 72300, Pueble, Mexico; yani.ramirez@utpuebla.edu.mx
* Correspondence: erick_gastellou@utpuebla.edu.mx or erick.gastellou@unison.mx; Tel.: +52-2224699594

check for updates

Citation: Gastellóu, E.; García, R.; Herrera, A.M.; Ramos, A.; García, G.; Hirata, G.A.; Luna, J.A.; Carrillo, R.C.; Rodríguez, J.A.; Robles, M.; et al. Hexagonal Nanocrystal Growth of Mg or Zn from Incorporation in GaN Powders Obtained through Pyrolysis of a Viscous Complex Compound and Its Nitridation. *Crystals* **2023**, *13*, 1421. https://doi.org/10.3390/cryst13101421

Academic Editors: Hongyu Yu and Qing Wang

Received: 10 September 2023
Revised: 16 September 2023
Accepted: 18 September 2023
Published: 25 September 2023

Copyright: © 2023 by the authors. Licensee MDPI, Basel, Switzerland. This article is an open access article distributed under the terms and conditions of the Creative Commons Attribution (CC BY) license (https://creativecommons.org/licenses/by/4.0/).

Abstract: Hexagonal nanocrystals were obtained from Zn-doped GaN powders and Mg-doped GaN powders, which were synthesized via pyrolysis of a viscous complex compound, followed by its nitridation. XRD showed well-defined peaks for hexagonal GaN with an average crystal size of 21.3 nm. Scanning electron microscopy showed an amorphous and porous appearance in surface morphology, which could be related to the combustion process. Energy-dispersive spectroscopy characterization showed contributions of gallium, nitrogen, and small traces of Zn and Mg in the GaN samples. TEM showed the presence of well-defined hexagonal nanocrystals with an area of 75.9 nm^2 for the Zn-doped GaN powders and an area of 67.7 nm^2 for the Mg-doped GaN powders. The photoluminescence spectra showed an emission energy of 2.8 eV (431.5 nm) for the Zn-doped GaN powders, while the Mg-doped GaN powders showed energies in the range from 2.7 eV to 2.8 eV (460.3 nm–443.9 nm). The Raman scattering showed spectra where the vibration modes A_1(TO), E_1(TO), and E_2(High) could be observed, which are characteristic of hexagonal GaN.

Keywords: powder; GaN; pyrolysis; crystal lattice; viscous complex compound

1. Introduction

Currently, the combustion synthesis (pyrolysis) of viscous complex compounds is an important technique to produce III-Nitride powder with high purity, single phase, and fine grain size [1,2]. This technique is based on a highly exothermic self-sustaining and self-propagating oxidation–reduction reaction between a reducing fuel and metal nitrates in a solution. The resulting material is a bulky and porous powder due to the large amount of gases that escape from the solid solution during the reaction. In these combustion synthesis processes, carbon-containing fuels such as carbohydrazide (CH_6N_4O) and urea ($(NH_2)_2CO$) are normally used. The reactions are carried out in an oven preheated to 100 °C open to atmosphere. Due to the fuels and the process conditions, the resulting materials frequently

present traces of carbon as a contaminating element, in addition to losses due to spills during combustion. On the other hand, in the III-Nitride compounds (GaN, AlN, and InN), the GaN stands out due to its optical and electrical properties. Gallium Nitride (GaN) was first synthesized in 1932 by Johnson, Parson, and Crew. Since then, researchers have focused their efforts on the GaN technology, to solve the problem that exists in the lattice mismatch of the material with respect to non-native substrates, as well as its p-type doping [3–5].

Economically, GaN has proven to be profitable for the telecommunications market with devices that operate at 5 W and below 3.8 GHz for WIMAX technology (IEEE 802.16e-2005-2.5 GHz). In this same field, NEC Electronics developed power transistors that operate at 45 V and 2.14 GHz for Toyoda Gosei. Other applications of GaN include solar cells, diode lasers, and LEDs [6,7]. The mechanical properties of GaN make it a very hard, very stable material, with a high heat conduction capacity and a direct band gap energy of 3.4 eV for the hexagonal structure (wurtzite) and 3.2 eV for the cubic structure (zinc blende). The technique most widely used in the semiconductors industry to obtain p-type GaN is metal–organic chemical vapor deposition (MOCVD). Although MOCVD is a proven technique for obtaining a large variety of materials, it is also a fact that this technique presents some difficulties, such as the high cost of metal–organic precursors and the delicate handling of gases, which, being pyrophoric, require special devices for their handling and storage. In addition, III-Nitrides present difficulties in the control of their type-p conductivity through the doping technique. Another technique recently used for thin-film deposition is magnetron RF sputtering, which can use targets made of Mg-doped or Zn-doped GaN powders. The powders can be obtained through the nitridation of powders previously doped with Mg or Zn [8].

This work presents the synthesis of Mg-doped GaN and Zn-doped GaN powders through combustion of a viscous complex compound followed by its nitridation at 1000 °C for two hours. The importance of this work is that the doping of GaN powders in this way still has not been reported in the literature. X-ray diffraction patterns (XRD) for Mg-doped GaN and Zn-doped GaN powders showed principal peaks for the wurtzite structure. Scanning electron microscopy (SEM) pictures for the Mg-doped GaN and Zn-doped GaN powders showed a porous surface morphology related to the combustion method. Mg or Zn elemental contributions to GaN powders were measured using energy-dispersive spectroscopy (EDS). Transmission electron microscopy (TEM) showed the presence of nanocrystallites, which generated the crystal structure in Mg-doped GaN and Zn-doped GaN powders. The photoluminescence (PL) spectrum showed broad peaks in the emissions in the blue band. On the other hand, Raman scattering demonstrated the presence of the principal vibration modes belonging to GaN powders.

2. Materials and Methods

The synthesis of Mg-doped GaN powders and Zn-doped GaN powders was performed at atmospheric pressure (785.9 mb). For the process of obtaining the Mg-doped GaN powders, carbohydrazide (CH_6N_4O), gallium nitrate $Ga(NO_3)_3$, and magnesium nitrate $Mg(NO_3)_2$ were used. To synthesize the Zn-doped GaN powders, carbohydrazide (CH_6N_4O), gallium nitrate $Ga(NO_3)_3$, and zinc nitrate $Zn(NO_3)_2$ were used. All reagents were of ultra-high purity and toluene was used as a solvent for nitrates and carbohydrazide. As a way to compare the results of Mg-doped GaN powders and Zn-doped GaN powders, undoped GaN powders were synthesized, which were prepared as presented in a previous work, Gastellóu et al. [2]. The reactions proposed to synthesize the Mg-doped GaN powders and Zn-doped GaN powders were the following:

$$Ga(NO_3)_3 + Mg(NO_3)_2 + (CH_6N_4O)_3 \rightarrow GaN{:}Mg(s) + H_2O(g) + CO(g) + N_2(g) \quad (1)$$

$$Ga(NO_3)_3 + Zn(NO_3)_2 + (CH_6N_4O)_3 \rightarrow GaN{:}Zn(s) + H_2O(g) + CO(g) + N_2(g) \quad (2)$$

The weights calculated to carry out the processes for obtaining the Mg-doped GaN powders were the following: 1.53266 g of carbohydrazide (CH_6N_4O), 2.06172 g of gallium nitrate $Ga(NO_3)_3$, and 21.23 mg of magnesium nitrate $Mg(NO_3)_2$ (2%). On the other hand, 1.53120 g of carbohydrazide (CH_6N_4O), 2.05978 g of gallium nitrate $Ga(NO_3)_3$, and 24.16 mg of zinc nitrate $Zn(NO_3)_2$ (2%) were weighed to synthesize the Zn-doped GaN powders. The following is a description of the synthesis process of the Mg-doped GaN powders and the Zn-doped GaN powders. Once the reagents were calculated and weighed on an analytical balance, the nitrates were placed inside a Teflon beaker, which was placed on a hot plate; the whole process was carried out in an extraction hood; the temperature of the hot plate was then increased to 60 °C; and 20 mL of toluene was poured in, turning on magnetic stirring. Later, the temperature was increased to 105 °C, and the moment the hot plate reached 85 °C, the carbohydrazide was added. Magnetic stirring was maintained for 40 min; during this time, the solution became a viscous complex compound, and then the Teflon beaker was removed from the hot plate and turned off to allow the compound to cool. Thereupon, a sample of no more than one gram was cut from the compound and placed in an alumina boat to be introduced into a CVD furnace to carry out the combustion process (pyrolysis). The sample was introduced into a CVD system, which was purged to remove residual contaminants, and then ultra-high-purity N_2 at 100 sccm was flowed as the combustion byproduct carry gas. Once this process was performed, the temperature was increased to 250 °C, which is the combustion temperature to obtain GaN [2]. When the temperature reached 250 °C, the sample was allowed to homogenize until it burned after 10 min, which was observed in the presence of white vapors [1]. Once combustion was reached, the system was raised to 1000 °C, where a flow of NH_3 at 100 sccm was opened and the flow of N_2 was closed. The nitridation process lasted two hours and, after this time, the N_2 flow was opened again at 100 sccm, the NH_3 flow was closed, and the heating control was turned off so that the room temperature would rise. When the material cooled, it was extracted from the CVD furnace and ground to carry out the corresponding characterizations.

Characterizations

The Mg-doped GaN powders and the Zn-doped GaN powders were characterized through X-ray diffraction patterns (XRD) using a Philips X'PERT MPD instrument with a wavelength (Cu Kα) of 1.5406 Å, in the range from 20 to 60 degrees. Surface morphology and elemental contributions (SEM-EDS) were characterized using a JEOL JSM-5300 instrument. On the other hand, transmission electron microscopy (TEM) was conducted using a JEOL-2010 instrument, while photoluminescence spectra (PL) were realized at room temperature with an excitation wavelength on a Hitachi F-7000 FL with a 150 W xenon lamp. Finally, Raman scattering was conducted using the Micro-Raman spectrophotometer Horiba Jobin Yvon HR-800.

3. Results and Discussion

3.1. Structural Analysis

Undoped and Mg or Zn-doped GaN powders were obtained through the pyrolysis route of a $Ga(NO_3)_3$-CH_6N_4O viscous complex compound followed by its nitridation in an ammonia flow at 1000 °C for two hours. Figure 1 shows the XRD of GaN powders without annealing (Figure 1a), annealed in an ammonia environment (Figure 1b), and doped with Mg or Zn (Figure 1c,d). Furthermore, Figure 1e shows the ICDD pdf card No. 00-050-0792 with which all diffraction patterns were indexed. The a peak was located in the (100) plane; b was located in (002); c, which had the greatest intensity, was located in (101); d was located in (102); and e was located in (110). The calculated lattice constants for the wurtzite structure were a = 3.19 Å and c = 5.18 Å, with a c/a ratio of 1.623. The unannealed powders showed an amorphous structure, which improved when thermal annealing in an ammonia environment at 1000 °C for two hours. In the different studies carried out, it was observed that at higher nitridation temperatures (1000 °C), there was

an enhancement in the crystalline structure of the GaN powders. The FWHM measure of the highest-intensity peak in the (101) plane was 0.40667°. Using the ICCD PDF-4+2022 software and the Debye–Scherrer equation, the crystal size was calculated, finding an average of 21.3 nm [9]. The broadening of the peaks in Figure 1 could be associated with the nature of the pyrolysis of the $Ga(NO_3)_3$-CH_6N_4O viscous complex compound, which generates a nitrogen deficiency in the GaN powders. These powders are composed of nanocrystallites, as demonstrated by Garcia et al. [1]. A nitrogen deficiency can introduce oxygen and carbon impurities, improving its nitrogen stoichiometry after NH_3 annealing.

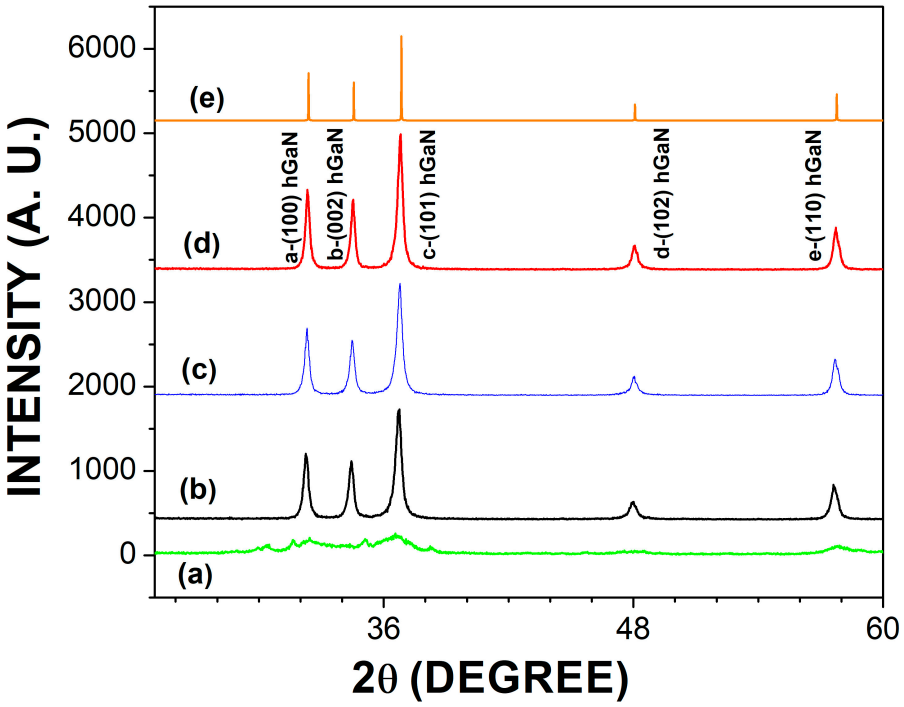

Figure 1. X-ray diffraction patterns: (**a**) unannealed GaN powders, (**b**) undoped GaN powders, (**c**) Zn-doped GaN powders, (**d**) Mg-doped GaN powders, and (**e**) ICDD pdf card No. 00-050-0792.

3.2. Electron Microscopy

Figure 2a shows the undoped and unannealed GaN powders, where a surface morphology with an amorphous and porous appearance can be observed, which could be related to nitrogen deficiency and the presence of non-intentional impurities such as oxygen due to the method of synthesis via combustion [2]. Figure 2e shows the gallium and oxygen contributions corresponding to Figure 2a. In Figure 2e, the nitrogen deficiency can also be observed, which agrees with what is mentioned in Figure 2a. Figure 2b shows the undoped GaN powders obtained through the pyrolysis of the $Ga(NO_3)_3$–CH_6N_4O viscous complex compound, annealed in an ammonia environment at 1000 °C for two hours. Figure 2b also presents a surface morphology with an amorphous appearance, which could again be related to nitrogen deficiency in this synthesis process and poor crystal growth. Figure 2f shows the elemental contributions of gallium and nitrogen, where it is also possible to observe the strong decrease in the oxygen contribution, which decreased due to thermal annealing, as well as the increase in nitrogen. Figure 2c shows the Mg-doped GaN powders. In this micrograph, the morphology presents a porous surface with agglomerates, as well as flat-like structures, which may be related to the accumulation of Mg in different areas of the material [10]. Figure 2g shows the elemental contributions of gallium, nitrogen, and a very small trace of magnesium, which is due to the fact that GaN has a very low concentration of this dopant element (~1%). Figure 2d shows the GaN powders doped with Zn, where, again, the amorphous and porous surface morphology stands out, while Figure 2h shows the contributions of gallium and nitrogen with a greater intensity concerning Figure 2a,b.

On the other hand, Figure 2d shows a very small contribution of Zn, which corresponds to 1% of the dopant incorporated into GaN [11].

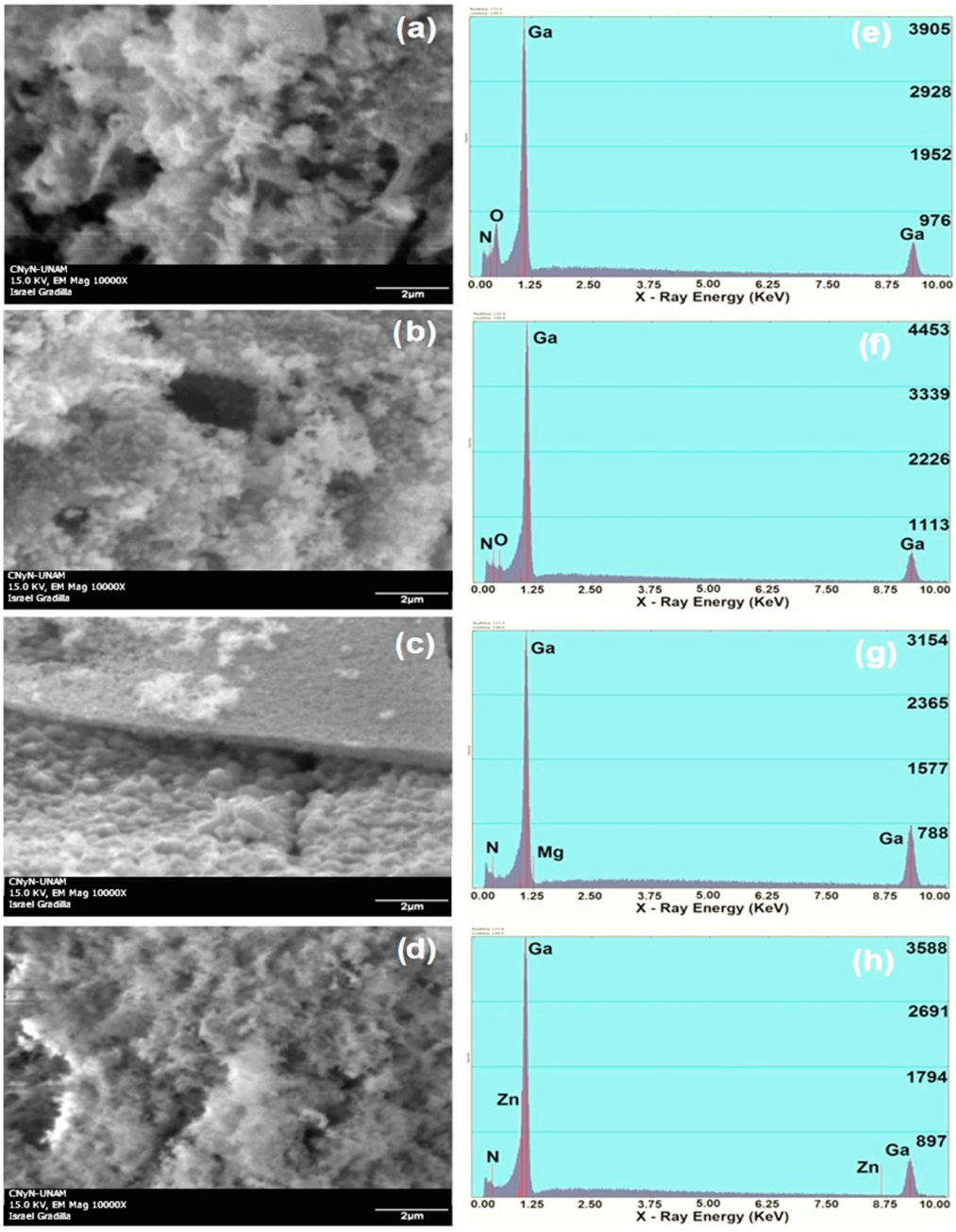

Figure 2. SEM-EDS micrographs: (**a**,**e**) unannealed GaN powders, (**b**,**f**) undoped GaN powders, (**c**,**g**) Mg-doped GaN powders, and (**d**,**h**) Zn-doped GaN powders.

Figure 3a presents the TEM picture, which shows the presence of hexagonal Zn-doped GaN nanocrystals. These hexagonal nanocrystals have dimensions per side of 149.1 nm and an area of 75.9 nm^2 at a magnification of 0.2 µm. Figure 3b shows the polycrystalline state of the Zn-doped GaN sample at 20 nm magnification, while Figure 3c presents the electron diffraction pattern, where it is possible to observe the hexagonal distribution for GaN, in addition to the difference in crystal size between GaN and the Zn dopant. Figure 3d also shows the presence of hexagonal nanocrystals of Mg-doped GaN, which are 145.9 nm per side and have an area of 67.7 nm^2 at a magnification of 0.2 µm. Figure 3e shows the polycrystalline state of the Mg-doped GaN sample at a

magnification of 20 nm, while Figure 3f again presents the difference between the crystal size of GaN and the dopant Mg.

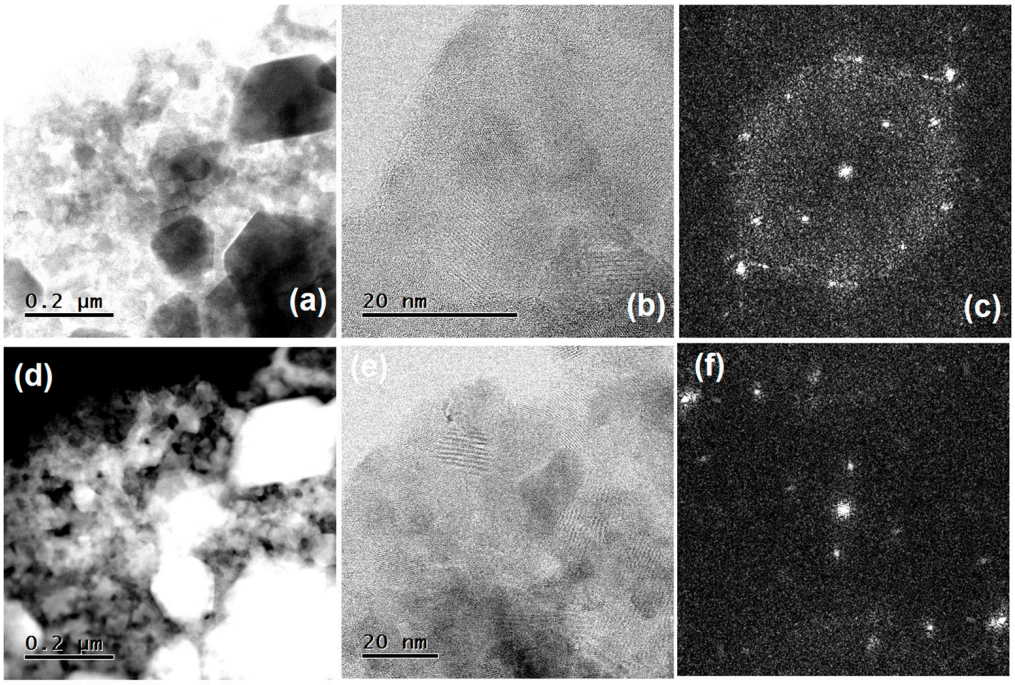

Figure 3. TEM micrographs: (**a**) hexagonal Zn-doped GaN nanocrystals, (**b**) polycrystalline state of the Zn-doped GaN powders, (**c**) electron diffraction pattern of Zn-doped GaN powders, (**d**) hexagonal Mg-doped GaN nanocrystals, (**e**) polycrystalline state of the Mg-doped GaN powders, and (**f**) electron diffraction pattern of Mg-doped GaN powders.

3.3. Photoluminescence

Figure 4 shows the photoluminescence spectra of the undoped and unannealed GaN powders, as well as the GaN powders annealed at 1000 °C for two hours in an ammonia flow. Furthermore, Figure 4 shows the energy emissions of the Zn-doped GaN powders as well as the Mg-doped GaN powders. In Figure 4, the d curve does not show an energy emission, which corresponds to undoped and unannealed GaN powders; this lack of energy emission agrees with the amorphous structure of Figure 1a. The a curve of Figure 4 corresponds to the emission of energy by the band-to-band transition of hexagonal GaN at 3.4 eV (365.5 nm). This well-defined energy emission is consistent with the XRD in Figure 1b.

In Figure 4, the b curve corresponds to the emission energy of Zn-doped GaN powders with a value of 2.8 eV (431.5 nm) [12]. In this energy emission, it is possible to observe a broad spectrum, which could be related to structural defects or non-intentional impurities in the material, generated during the combustion process. The c emission of energy in Figure 4 corresponds to the Mg-doped GaN powders, in which it is also possible to observe a broad spectrum in a range of 2.7 eV–2.8 eV (460.3 nm–443.9 nm) [12]. For higher wavelengths (600 nm–700 nm), defects such as non-intentional impurities (oxygen) are present in the emissions of Zn-doped GaN powders and Mg-doped GaN powders.

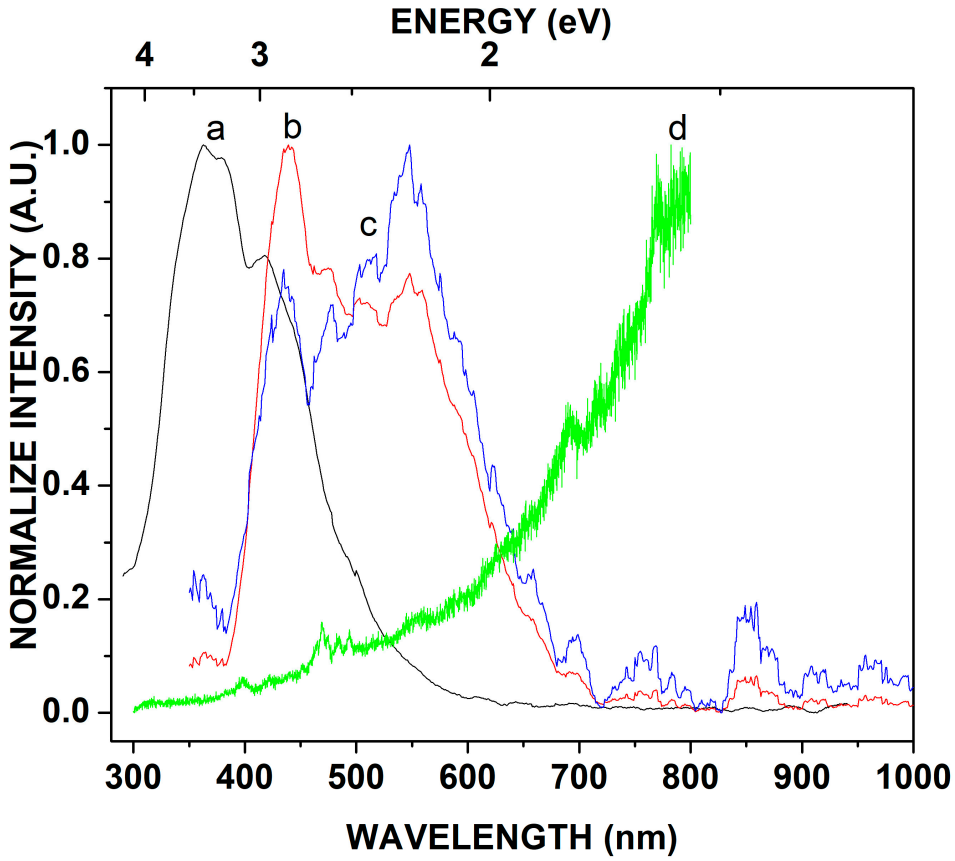

Figure 4. Photoluminescence spectra for a—undoped GaN powders; b—Zn-doped GaN powders; c—Mg-doped GaN powders; and d—unannealed GaN powders.

3.4. Raman Scattering

The Raman scattering spectra obtained for the GaN powders synthesized through pyrolysis of the $Ga(NO_3)_3$-CH_6N_4O viscous complex compound, followed by its nitridation in an ammonia environment at 1000 °C for two hours, are shown in Figure 5. Figure 5a shows the spectrum for unannealed and undoped GaN powders, while Figure 5b shows the spectrum for undoped and annealed GaN powders for 2 h in ammonia. Figure 5c shows the spectrum for the Zn-doped GaN powders, and Figure 5d also shows the spectrum for the Mg-doped GaN powders. In general, in the dispersion spectra, it is possible to identify three characteristic Raman vibration modes for hexagonal GaN with frequencies of 527.25 cm^{-1}, 556.18 cm^{-1}, and 564.03 cm^{-1}. For unannealed GaN powders, a lower definition of the three vibration modes is presented. The phononic vibration frequencies correspond to the modes A_1(TO), E_1(TO), and E_2(High) for the hexagonal wurtzite structure of GaN [13]. It is important to note that the introduction of the Zn and Mg dopant atoms had no effect on the vibration frequency of the A_1(TO), E_1(TO), and, especially, E_2(High) modes, which is because the atomic radii of gallium, zinc, and magnesium are very similar, which agrees with Figure 1, in the X-ray diffraction patterns, which also have no shifts in their reflection angles [14]. On the other hand, the undoped GaN powders appear slightly wider toward high frequencies, due to the possible incorporation of the non-intentional impurity of oxygen, which could increase their vibration frequency compared to the GaN powders doped with Zn or Mg. This agrees with the EDS and photoluminescence characterizations for the non-intentional oxygen impurities.

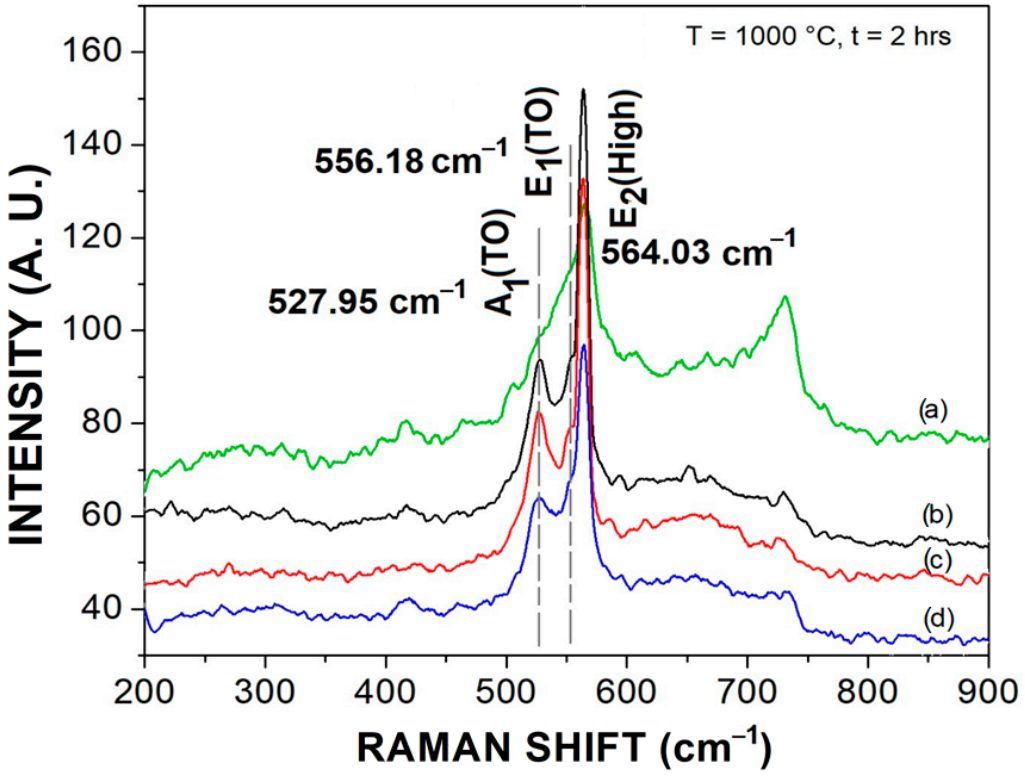

Figure 5. Raman scattering spectra for (**a**) unannealed and undoped GaN powders, (**b**) undoped and annealed GaN powders, (**c**) Zn-doped GaN powders, and (**d**) Mg-doped GaN powders.

4. Conclusions

Hexagonal nanocrystals were found in Zn-doped GaN powders and Mg-doped GaN powders, which were synthesized through the pyrolysis route of a $Ga(NO_3)$-CH_6N_4O viscous complex compound followed by its nitridation in a flow of ammonia at 1000 °C for two hours. The XRD showed well-defined peaks for hexagonal GaN with an average crystal size of 21.3 nm. SEM pictures generally showed an amorphous and porous appearance in surface morphology, which could be related to the combustion process during the synthesis. On the other hand, EDS characterization showed contributions of gallium, nitrogen, and small traces of Zn and Mg in the GaN powder samples. TEM showed the presence of well-defined hexagonal nanocrystals with an area of 75.9 nm^2 for the Zn-doped GaN powders and an area of 67.7 nm^2 for the Mg-doped GaN powders. The photoluminescence spectra showed an emission energy of 2.8 eV (431.5 nm) for the Zn-doped GaN powders, while the Mg-doped GaN powders showed an emission energy in the range from 2.7 eV to 2.8 eV (460.3 nm–443.9 nm). Finally, Raman scattering showed spectra where the vibration modes A_1(TO), E_1(TO), and E_2(High) could be observed, which are characteristic of hexagonal GaN.

Author Contributions: Conceptualization, E.G.; Methodology, Formal Analysis, Investigation, Writing—Original Draft, Resources, R.G.; Formal Analysis, Investigation, Writing—Original Draft, A.M.H.; Resources, A.R.; Conceptualization, G.G.; Resources, G.A.H.; Resources, J.A.L.; Resources, R.C.C.; Writing—Original Draft, J.A.R.; Resources, M.R.; Validation, Y.D.R. All authors have read and agreed to the published version of the manuscript.

Funding: This research received no external funding.

Institutional Review Board Statement: Not applicable.

Informed Consent Statement: Not applicable.

Data Availability Statement: Data are contained within the article.

Acknowledgments: The authors gratefully acknowledge the technical support of CNyN-UNAM, particularly Eloísa Aparicio, Israel Granilla, and Oscar Edel Contreras. This research was partially supported by CONACyT (México) and DIFUS-UNISON.

Conflicts of Interest: The authors declare no conflict of interest.

References

1. Garcia, R.; Hirata, G.A.; Thomas, A.C.; Ponce, F.A. Structure and luminescence of nanocrystalline gallium nitride synthesized by a novel polymer pyrolysis route. *Opt. Mater.* **2006**, *29*, 19–23. [CrossRef]
2. Gastellou, E.; Morales, C.; García, R.; García, G.; Hirata, G.A.; Galeazzi, R.; Herrera, A.M.; Rosendo, E.; Díaz, T.; Ramos, J.R.; et al. Enhanced crystalline size of undoped GaN powders obtained by nitridation of metallic gallium. *Opt. Mater.* **2018**, *83*, 154–196. [CrossRef]
3. Benzarti, Z.; Sekrafi, T.; Bougrioua, Z.; Khalfallah, A.; El Jani, B. Effect of SiN Treatment on Optical Properties of $In_xGa_{1-x}N$/GaN MQW Blue LEDs. *J. Electron. Mater.* **2017**, *46*, 4312–4320. [CrossRef]
4. Benzarti, Z.; Khalfallah, A.; Bougrioua, Z.; Evaristo, M.; Cavaleiro, A. Understanding the influence of physical properties on the mechanical characteristics of Mg-doped GaN thin films. *Mater. Chem. Phys.* **2023**, *307*, 128182. [CrossRef]
5. Escobosa, A.; Sánchez-R, V.M.; To, M.; Navarro, A.G. Photoluminescence studies of GaN: To comparison between layers grown on sapphire and nitridated GaAs layers. *Phys. Status Solidi B* **2005**, *242*, 1883–1886. [CrossRef]
6. Sim, J.K.; Um, D.Y.; Kim, J.W.; Kim, J.S.; Jeong, K.U.; Lee, C.R. Improvement in the performance of CIGS solar cells by introducing GaN nanowires on the absorber layer. *J. Alloys Compd.* **2019**, *779*, 643–647. [CrossRef]
7. Amano, H.; Baines, Y.; Beam, E.; Borga, M.; Bouchet, T.; Chalker, P.R.; Charles, M.; Chen, K.J.; Chowdhury, N.; Chu, R.; et al. The 2018 GaN power electronics roadmap. *J. Phys. D Appl. Phys.* **2018**, *51*, 163001. [CrossRef]
8. Maruyama, T.; Miyake, H. Gallium nitride thin films deposited by radio-frequency magnetron sputtering. *J. Vac. Sci. Technol. A* **2006**, *4*, 1096–1099. [CrossRef]
9. Langford, I.; Wilson, A.J.C. Sherrer after sixty years: A survey and some new results in the determination of crystallite size. *J. Appl. Crystallogr.* **1978**, *11*, 102–113. [CrossRef]
10. Ilegems, M.; Dingle, R. Luminescence of Be- and Mg-doped GaN. *J. Appl. Phys.* **1973**, *44*, 4234–4235. [CrossRef]
11. Pankove, J.I.; Berkeyheiser, J.E.; Miller, E.A. Properties of Zn-doped GaN. I. Photoluminescence. *J. Appl. Phys.* **1974**, *45*, 1280–1286. [CrossRef]
12. Reshchikov, M.A.; Morkoç, H. Luminescence properties of defects in GaN. *J. Appl. Phys.* **2005**, *97*, 061301. [CrossRef]
13. Kumar, M.S.; Kumar, J. XRD, XPS, SEM, PL and Raman scattering analysis ofsynthesized GaN powder. *Mater. Chem. Phys.* **2002**, *77*, 341–345. [CrossRef]
14. Kuball, M. Raman spectroscopy of GaN, AlGaN and AlN for process and growth monitoring/control. *Surf. Interface Anal.* **2001**, *31*, 987–999. [CrossRef]

Disclaimer/Publisher's Note: The statements, opinions and data contained in all publications are solely those of the individual author(s) and contributor(s) and not of MDPI and/or the editor(s). MDPI and/or the editor(s) disclaim responsibility for any injury to people or property resulting from any ideas, methods, instructions or products referred to in the content.